Enhanced Binding of the TATA-Binding Protein to TATA Boxes Containing Flanking Cisplatin 1,2-Cross-Links†

Seth M. Cohen,‡ Elizabeth R. Jamieson,§ and Stephen J. Lippard*

Department of Chemistry, Massachusetts Institute of Technology, Cambridge, Massachusetts 02139

Received February 28, 2000; Revised Manuscript Received April 11, 2000

ABSTRACT: The TATA-binding protein (TBP) is essential for transcription initiation in eukaryotes. TBP recognizes and binds to the minor groove of a consensus sequence, TATAAA, known as the TATA box or TATA element. DNA binding is affected largely by hydrophobic contacts and through the intercalation of two sets of adjacent phenylalanine residues. The resultant duplex is sharply kinked, bending toward the major groove. Inspired by prior structural information showing intercalation of a phenylalanine side chain of a high mobility group (HMG) domain into the site of a cisplatin 1,2-intrastrand d(GpG) cross-link, a series of DNA probes was prepared with one or two such adducts flanking the TATA box positions at or near the sites of TBP intercalation. The platinum adducts bend the DNA toward the major groove and result in as much as a 175-fold increase in binding affinity of the TBP over the unmodified target sequence. Kinetic studies indicate that the enhanced binding to the modified TATA box is predominantly a consequence of a >30-fold slower dissociation rate of the protein−platinated DNA complex. This work demonstrates that it is feasible to design rationally and to synthesize an enhanced affinity-binding site for a sequence-specific DNA-binding protein by appropriate chemical modification of flanking sequences. It also has implications for the mechanism of action of cisplatin.

The TATA-binding protein (TBP)[1] is one member of the TFIID protein assembly involved in eukaryotic transcription initiation (*1*). TBP recognizes and binds to the consensus sequence TATAAA that is typically located 25−30 base pairs upstream of a transcription start site. Studies of the TBP−DNA complex show that TBP binds the TATA box from the minor groove of the DNA, largely through a hydrophobic β-sheet surface and four intercalating residues. For yeast TBP (yTBP) four phenyalanine side chains, two each on either side of the consensus sequence, unwind and bend the DNA (*2*−*6*).

The predominantly hydrophobic interaction of the protein with the minor groove of the DNA duplex leads to the hypothesis that the TATA box is recognized owing to the deformability of the sequence rather than a base-specific readout (*2*). This proposal has been supported in part by structural information, including the low number of base-specific contacts in TBP−DNA complexes, and by calculations on the DNA sequence. Several studies have demonstrated that structurally modified TATA sequences modulate TBP binding. Bending the TATA box toward the major groove in a circularized DNA containing properly positioned A-tracts enhanced TBP binding ~100-fold, whereas a sequence bent toward the minor groove exhibited reduced TBP binding (*7*). Adding flexibility by introducing base pair mismatches at flanking positions on either side of the TATA box also enhanced TBP binding (*8*). The use of 5-hydroxymethyluracil in place of thymine in the TATA element also increased flexibility and resulted in enhanced TBP binding (*8*).

The high-mobility group (HMG) domain proteins are another class of DNA-binding proteins that recognize bent DNA structures including cruciform and cisplatin-damaged DNA (*9*). Like TBP, HMG domain proteins bind DNA through the minor groove. Several HMG proteins specifically recognize the major adducts of the anticancer drug cisplatin 1,2-d(ApG) and 1,2-d(GpG) cross-links (*10*, *11*). The binding of HMG domain proteins to cisplatin-modified DNA may play an important role in mediating the biological activity of the drug by one or more of several pathways (*12*). Recently, the X-ray crystal structure of an HMG domain complexed with a cisplatin-modified DNA was reported (*13*). This structure revealed that recognition of the DNA lesion occurs through minor groove interactions that include intercalation of a phenylalanine residue between the two guanine bases bound to the platinum atom. Mutation of the phenylalanine to alanine markedly reduced the affinity of the domain for cisplatin-modified DNA. Like the HMG domain proteins, TBP binds to cisplatin-modified DNA and

† Supported by Grant CA34992 from the National Cancer Institute. This paper is dedicated to the memory of Prof. Paul Sigler of Yale University.

* To whom correspondence should be addressed. Telephone: (617) 253-1892. Fax: (617) 258-8150. E-mail: lippard@lippard.mit.edu.

‡ Recipient of a National Institutes of Health postdoctoral fellowship.

§ Recipient of an ACS Medicinal Chemistry graduate fellowship.

[1] Abbreviations: EMSA, electrophoretic mobility shift assay; HMG, high-mobility group; PAGE, polyacrylamide gel electrophoresis; TBP, TATA-binding protein; TFII, transcription factor two; yTBP, yeast TATA-binding protein; hTBP, human TATA-binding protein; *cis*-diamminedichloroplatinum(II); bp, base pair; *E. coli*, *Escherichia coli*; HEPES, *N*-[2-hydroxyethyl]piperazine-*N*′-[2-ethanesulfonic acid]; Tris, tris-[hydroxymethyl]aminomethane; HPLC, high performance liquid chromatography; BSA, bovine serum albumin; DTT, dithiothreitol; EDTA, ethylenediaminetetraacetic acid; PIC, preinitation complex.

10.1021/bi0004495 CCC: $19.00
Published on Web 06/17/2000

also may play a role in potentiating its biological activity (*14*, *15*).

Bending of the TATA box upon TBP binding is an important factor in stabilizing the protein−DNA complex and initiating transcription (*16*). Several similarities exist between the interactions of TBP with the TATA box and HMG domains with cisplatin-modified DNA, including bending and unwinding of the DNA, recognition of a widened and flattened minor groove, and strong intercalative interactions. We were therefore interested to explore whether cisplatin modification in the vicinity of a TATA box would result in enhanced binding of TBP and how the positioning of the adduct(s) would affect the results. Herein we report a series of cisplatin-modified TATA boxes that form substantially stronger TBP complexes when compared to unmodified TATA sequences. The results indicate that intercalation is critical for the interaction of the TBP with cisplatin-modified DNA.

EXPERIMENTAL PROCEDURES

Protein Preparation. Human transcription factor two B (hTFIIB) and full-length human TATA-binding protein (hTBP), provided as a gift by Prof. P. A. Sharp and Dr. D. Dykxhoorn, were expressed and purified by literature methods (*17*). The yeast TATA-binding protein (yTBP) was expressed from a previously reported plasmid encoding for the 179-amino acid C-terminus of protein (*18*). The plasmid was transformed via electroporation into BL21(DE3) *Escherichia coli* cells for expression. Cells were grown in minimal media (10 × 500 mL cultures) inoculated with 75 mg/mL ampicillin (500 μL/culture, Sigma). All subsequent manipulations were carried out at 4 °C, and all buffers contained 1 mM DTT, 0.1 μM pepstatin A, 0.03 μM leupeptin, 0.16 μM chymostatin, 0.1 mM benzamidine (Sigma), and 0.01 μM Pefabloc. The inhibitors were obtained from Boehringer-Mannheim (except where indicated) and prepared as a 100× stock solution in ethanol. All purification steps were monitored by 4−20% Tris-HCl SDS−PAGE (Bio-Rad) with Coomassie staining. The cells were isolated by centrifugation and sonicated in lysis buffer (50 mM Tris, pH 8.0, 400 mM NaCl, 1 mM EDTA, and 10% glycerol). The sonicated mixtures were centrifuged, and the supernatant was allowed to react slowly (20 min) with protamine sulfate (0.04%). The solution was centrifuged, and the supernatant treated with ammonium sulfate (47 g/mL). The slurry was centrifuged, and the pellet was redissolved in HEPES buffer (50 mM HEPES, pH 7.5, 0.1 mM EDTA, and 10% glycerol). The solution was loaded onto a 10-mL heparin-Sepharose column (Bio-Rad) and rinsed with HEPES buffer containing 100 mM followed by 300 mM KCl. The protein was eluted by washing with HEPES buffer containing 600 mM KCl. The pooled fractions were treated with ammonium sulfate (47 g/mL) over 20 min. The liquid was decanted away and centrifuged. The resulting pellet was redissolved in Tris buffer (50 mM Tris, pH 8.0, 0.1 mM EDTA, and 10% glycerol) containing 100 mM KCl. The solution was loaded onto a 250-mL Sephadex G-50 column (Pharmacia Biotech) and eluted with Tris buffer containing 100 mM KCl. The desired fractions were pooled and loaded onto a 10-mL Q-Sepharose column (Bio-Rad) and eluted with Tris buffer containing 100 mM KCl. The desired fractions were pooled and loaded onto an 8-mL SP-Sepharose column (Pharmacia Biotech) that was washed with HEPES buffer containing 100 mM followed by 200 mM KCl. The protein was eluted with HEPES buffer and a gradient of 200 to 800 mM KCl over 80 min. The purified protein was washed and concentrated by using an Ultrafree-15 Centrifugal filter (5000 MWCO, Millipore). The protein was stored in storage buffer (HEPES 10 mM, pH 7.5, 25 mM KCl, and 1 mM DTT, no protease inhibitors).

Table 1: Probe Sequences and Codes

codes[a]	variable portion of oligonucleotide sequence[b]
[−5,+5]	5′. . . −CCG G TTATAAACG G TCC- . . . 3′
Pt_2[−5,+5]	5′. . . −CCG*G*TTATAAACG*G*TCC− . . . 3′
[−4,+5]	5′. . . −CCTG G TATAAACG G TCC- . . . 3′
Pt_2[−4,+5]	5′. . . −CCTG*G*TATAAACG*G*TCC− . . . 3′
[−3,+5]	5′. . . −CCTTG G ATAAACG G TCC- . . . 3′
Pt_2[−3,+5]	5′. . . −CCTTG*G*ATAAACG*G*TCC− . . . 3′
[−4,+4]	5′. . . −CCTG G TATAAAG G CTCC- . . . 3′
Pt_2[−4,+4]	5′. . . −CCTG*G*TATAAAG*G*CTCC− . . . 3′
^{3}Pt[−4,+4]	5′. . . −CCTG G TATAAAG*G*CTCC- . . . 3′
^{5}Pt[−4,+4]	5′. . . −CCTG*G*TATAAAG G CTCC− . . . 3′

[a] Codes refer to the position (in base pairs) of the GG sites relative to the central *TA base pair step* of the TA*TA*AA consensus sequence. [b] G*G* indicates a cisplatin 1,2-intrastand adduct. Complete sequences are provided as Supporting Information.

Total protein concentrations were determined with the use of a Coomassie dye assay (Pierce). The final yield from 10 L of culture was 12.4 mg. Active protein concentration was determined, by titration with an excess of the [−4,+4] (vide infra) probe oligonucleotide (*19*), to be approximately 27 ± 4% of the total protein concentration. All reported concentrations indicate active protein concentration unless specified otherwise.

Oligonucleotide Probes. Duplex DNA probes (55 bp) were constructed from three (for [−N,+N] or Pt_2[−N,+N] probes) or four (^{3}Pt[−4,+4] and ^{5}Pt[−4,+4] probes) smaller component oligonucleotides synthesized on a Applied Biosystems 392 DNA/RNA synthesizer using standard phosphoramidite methods (Table 1). Component oligonucleotides were purified on denaturing polyacrylamide gels (7.5 M urea, 19:1 acrylamide/bisacrylamide, 90 mM Tris−borate, and 1.0 mM EDTA, pH 8.3) run at constant voltage (300 V) cooled to ambient room temperature.

For the [−N,+N] or Pt_2[−N,+N] oligonucleotide probes, an 18-mer, 37-mer (containing the TATA box and GG sites), and 55-mer were synthesized. The 18-mer (0.02 μmol) was phosphorylated on the 5′-end by using 800 U of T4 polynucleotide kinase (New England Biolabs) in a solution (1 mL) containing 1× kinase buffer (supplied with the enzyme) and 15 mM ATP. The mixture was incubated at 37 °C for 45 min followed by addition of another 800 U of T4 polynucleotide kinase. After a second incubation at 37 °C for 45 min, the reaction mixture was extracted with 2 × 1 mL of 25:24:1 phenol/$CHCl_3$/isoamyl alcohol. The phosphorylated oligonucleotide was finally isolated by ethanol precipitation. The phosphorylated 18-mer was mixed with the 37-mer (platinated or unplatinated) and annealed to the corresponding 55-mer by heating to 90 °C for 4 min followed by cooling to 4 °C over several hours in a solution (100 μL) containing 50 mM Tris (pH 7.9), 10 mM $MgCl_2$, 100 mM NaCl, and 1 mM DTT. The annealed mixtures were then made 2.8 mM in ATP and 60 μg/mL in BSA followed by addition of 6000 U of T4 DNA ligase (New England

Biolabs). The mixtures (250 μL) were left at room temperature for 45 min followed by incubation at 16 °C overnight. The solutions were then extracted with 2 × 250 μL of 25:24:1 phenol/$CHCl_3$/isoamyl alcohol, and the DNA was isolated by ethanol precipitation. Aliquots of the isolated DNA were radiolabeled (vide infra) and run in parallel next to the unlabeled DNA on a 12% denaturing polyacrylamide gel (300 V, 50 °C). The gels were visualized by autoradiography, and the film was used as a guide to locate and excise the 55-mer bands. The isolated DNA was reannealed in 10 mM Tris, 50 mM NaCl, and 10 mM $MgCl_2$ in a volume of 50 μL. Aliquots (2 μL) of the annealed solutions were radiolabeled and run in parallel next to the unlabeled DNA on 12% native polyacrylamide gels (300 V). The gels were visualized by autoradiography, and the film was used as a guide to locate and excise the purified 55-base pair probes.

Gel Mobility Shift Assays. General Methods. Oligonucleotides were radioactively labeled in a solution (20 μL) containing 70 mM Tris-HCl, pH 7.6, 10 mM $MgCl_2$, 5 mM DTT, and 40 μCi of γ-^{32}P-labeled (Dupont/NEN). The oligonucleotide solutions were mixed with 10 U of T4 polynucleotide kinase (New England Biolabs) and incubated at 37 °C. After 45 min, 10 U of T4 polynucleotide kinase was added, and the mixtures were incubated at 37 °C for another 45 min. The reaction mixtures were spin-dialyzed through G-25 Sephadex Quickspin columns (Boehringer-Mannheim). The effluents were diluted with water to a total volume of 100 μL followed by extraction with 2 × 100 μL of 25:24:1 phenol/$CHCl_3$/isoamyl alcohol. The labeled probes were isolated by ethanol precipitation. Oligonucleotide probes (10 000 cpm/μL) and yTBP (19 ng/μL, total protein) were incubated at various relative concentrations in a buffered solution containing 60 mM KCl, 20 mM Tris (pH 7.9), 5.0 mM $MgCl_2$, 10 mM DTT, 0.2 mg/mL BSA, and 10% glycerol. Reactions were incubated at 30 °C for 0−60 min (see below) prior to electrophoresis. Native polyacrylamide gels (10%) were prepared and run in a buffer containing 25 mM Tris (pH 7.9), 190 mM glycine, 1.0 mM EDTA, and 4.0 mM $MgCl_2$. Gels were pre-run at constant voltage (140 V), with cooling for at least 30 min before loading of samples. After loading of samples, electrophoresis was continued for a minimum of 3.0 h to obtain satisfactory resolution. Gels were dried at 80 °C under vacuum for 1.0−1.5 h and subsequently exposed to a phosphorimaging plate overnight. Images were recorded by using a Bio-Rad GS-525 Molecular Imager and quantified with the Multianalyst software package.

Dissociation Rate Constants (*7*). To determine complex dissociation rate constants in solution (k_{off}), reaction mixtures (250 μL) containing 0.55−0.75 nM probe DNA and 6 nM yTBP were incubated at 30 °C. After 30−60 min, the reaction mixtures were quenched with 3.2 μg of poly[dI·dC]. Aliquots (20 μL) were removed at various time points after the addition of competitor and subjected to electrophoresis. The rate of dissociation was monitored by disappearance of the band corresponding to the yTBP−DNA complex. The amount of complex present (θ) at time t was fit under first-order conditions (eqs 1 and 2). The natural log of the amount of complex, normalized to the beginning of the reaction, eq 2, versus time was graphed and fit to a least-squares linear regression (Kaleidagraph). The k_{off} value was obtained from the negative slope of the fit.

$$[\text{complex}] = [\text{complex}]_0 e^{-k_{off}t} \quad (1)$$

$$\ln\frac{[\text{complex}]}{[\text{complex}]_0} = -k_{off}t \quad (2)$$

Association Rate Constants (*7*). To determine the complex association rate constants (k_{on}), reaction mixtures (250 μL) containing 0.25−0.5 nM probe DNA were equilibrated at 30 °C followed by addition of 6 nM yTBP. After addition of protein, aliquots (20 μL) were removed at various time points, quenched with 200 ng poly[dI·dC], and immediately subjected to electrophoresis. The rate constant was obtained by analyzing the first 2−3 min of the reaction according to eqs 3 and 4. The disappearance of free DNA probe (eq 4) was plotted versus time, and the data were fit to a linear regression giving k_{on} as the slope of the fit (Kaleidagraph).

$$\text{rate} = k_{off}[\text{complex}] - k_{on}[\text{TBP}][\text{unbound DNA}] \quad (3)$$

$$\frac{1}{[\text{yTBP}]}\ln\frac{[\text{unbound DNA}]}{[\text{unbound DNA}] - [\text{complex}]} = k_{on}t \quad (4)$$

RESULTS

Cisplatin-Modified Flanking Sequences Enhance yTBP Binding. Four 55-bp sequences were prepared for study with yTBP. The four oligonucleotides were used to generate 10 different probes: four unmodified probes, four probes with cisplatin adducts flanking both sides of the TATA element, and two probes with single cisplatin lesions either to the 5′- or 3′-side of the TATA consensus sequence. The probes were constructed according to the scheme presented in Figure 1. For platinated probes, the adducts were always located on the strand containing the TATA consensus sequence. Table 1 provides a complete list of probes including nomenclature codes and consensus sequences.

yTBP binding is notably enhanced by the presence of cisplatin adducts. As shown in Figure 2, under conditions where yTBP interacts weakly with a TATA element, binding to the platinum-modified probe is much stronger. A qualitative comparison of the different 55-bp probes demonstrates a strong preference for the platinated sequences. Figure 3A plots the fraction (θ) of bound DNA for each oligonucleotide at a constant protein concentration, revealing a substantial binding enhancement for the platinum-containing probes. For all sequences examined, platination affords a 2−6-fold increase in the fraction of bound DNA. The enhancement is more clearly illustrated (Figure 3B) by plotting the ratio (ρ) of θ values for the platinated versus the unplatinated probes.

Restored Binding to a Mutated TATA Element. In the qualitative analysis provided by Figure 3, the largest ρ-value occurs for the [−3,+5] probe, the sequence of which contains 5′-... CCTTGGATAAACGGTCC... −3′. Of the probes investigated, only [−3,+5] contains a mutated TATA box. Under optimized conditions, yTBP displays only a very weak bandshift with [−3,+5], a result consistent with the weak transcriptional activity of the GATAAA box (*2*, *20*). The cisplatin-modified probe Pt_2[−3,+5], consensus sequence 5′-... CCTTG*G*ATAAACG*G*TCC... −3′, where G*G* indicates a single cisplatin 1,2-intrastrand adduct, exhibits a ∼6-fold increase in the fraction of bound DNA. This enhancement is greater than that observed for any of the other

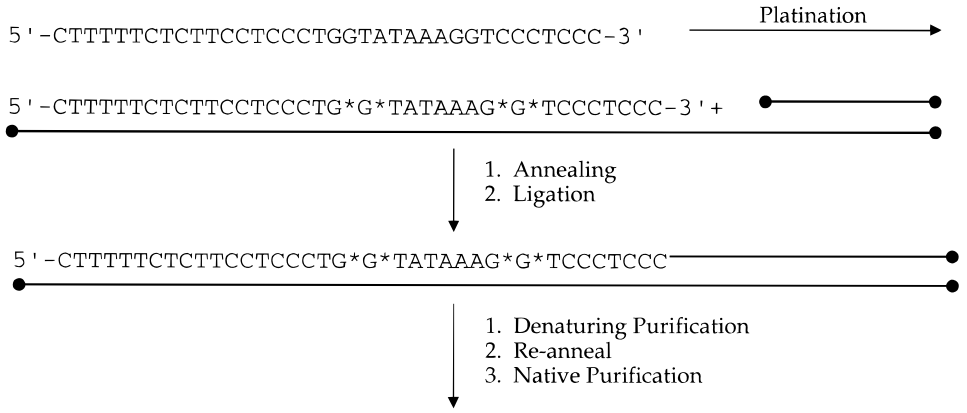

FIGURE 1: Synthetic scheme for oligonucleotide probes. 37-mer TATA box sequences were platinated at the GG sites. The platinated 37-mer was combined with an 18-mer and annealed to a 55-mer bottom strand. The 37-mer and 18-mer were ligated to make a 55-mer top strand followed by denaturing polyacrylamide gel electrophoresis (PAGE). The 55-mers were then reannealed and purified by native PAGE. Unplatinated probes were prepared in the same fashion without platination of the 37-mer. Monoplatinated probes were synthesized in an identical fashion using two components to make the 37-mer fragment (see Supporting Information).

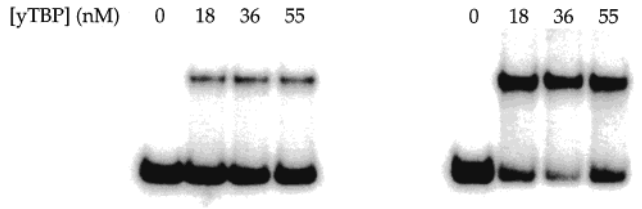

FIGURE 2: Electrophoretic mobility shift assay (EMSA) of [−4,+4] (left) and Pt_2[−4,+4] (right) with increasing amounts of yTBP. The unmodified probe [−4,+4] forms a stable complex, but enhancement is apparent when compared to the platinated probe Pt_2[−4,+4]. The first lane is a control that does not contain protein.

probes, all of which contain wild-type TATA boxes. Binding of yTBP to Pt_2[−3,+5] is stronger than observed for any of the unplatinated wild-type probes.

Measurement of Association Rate Constants. The association rate constants of yTBP binding to various oligonucleotide probes were determined by kinetic EMSA analysis (*7*, *21*). As shown in Figure 4, formation of a yTBP−DNA complex occurs within 1 min after protein addition. No correction was applied for dissociation during electrophoresis, which is unnecessary for C-terminal truncated forms of the protein (*22*). Platinum-modified probes display a 3−5-fold enhancement in association rate constant as compared to the unmodified probes (Table 2).

Measurement of Dissociation Rate Constants. EMSA was used to determine the solution dissociation rate constants for the yTBP−DNA complexes (*7*, *8*, *21*). Figure 5 shows representative EMSA data used to determine dissociation rate constants as well as the kinetic analysis. A large difference in dissociation rate is observed for unplatinated versus platinated probes.

Probes containing platinum adducts in the [−N,+4] position exhibited the largest change in dissociation rates, with constants ∼35-fold less than the unplatinated consensus sequence probes. The Pt_2[−4,+4] and ^{3}Pt[−4,+4] probes contain a platinum adduct exactly at the sites of intercalation for phenylalanine residues F99 and F116. Probes with platinum adducts one base pair from the site of intercalation on the 5′-side of the TATA box also show a dramatic (20−25-fold) decrease in dissociation rate constant. When the platinum adduct is placed farther from the TATA box (Pt_2[−5,+5]), the effect is diminished, providing only a

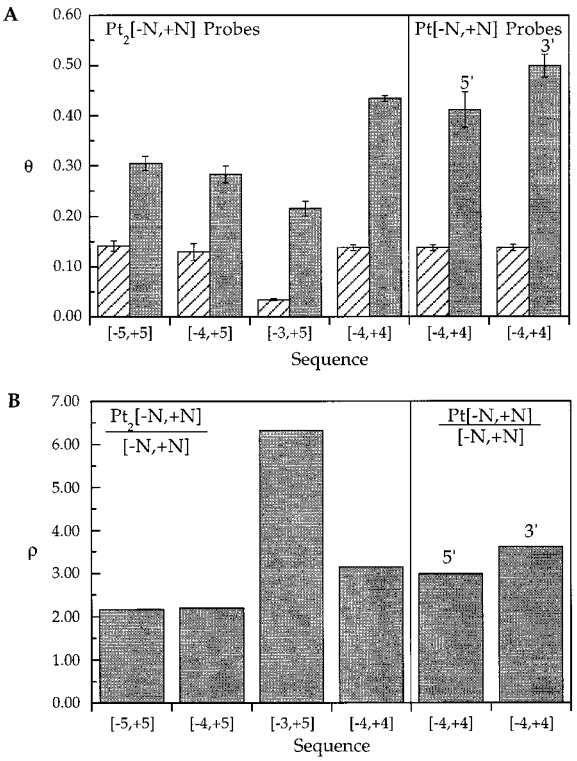

FIGURE 3: Panel A shows the fraction of bound probe DNA (θ) determined by EMSA. Hatched bars represent unplatinated 55-bp oligonucleotides, and filled bars represent platinated sequences (Pt_n[−N,+N]). Error bars represent one standard deviation obtained from the analysis of at least four independent experiments. Panel B shows the ratio (ρ) of bound DNA for platinated versus the unplatinated probes. Oligonucleotide concentrations were 0.25−0.5 nM with 18 nM yTBP.

2-fold decrease in k_{off} when compared to the unplatinated oligonucleotide.

Determination of Dissociation Constants. The kinetic parameters for binding of yTBP were used to determine dissociation constants ($K_d = k_{off}/k_{on}$) in a manner similar to that used in several other studies (*7*, *8*, *21*). Differences in affinity were dominated by variations in the dissociation rate constant. Association rate constants varied much less between probes (vide supra). The unplatinated probes had nearly identical dissociation rate constants of $1.2(1) \times 10^{-4}$ s^{-1}. This value compares well with others in the literature (*7*,

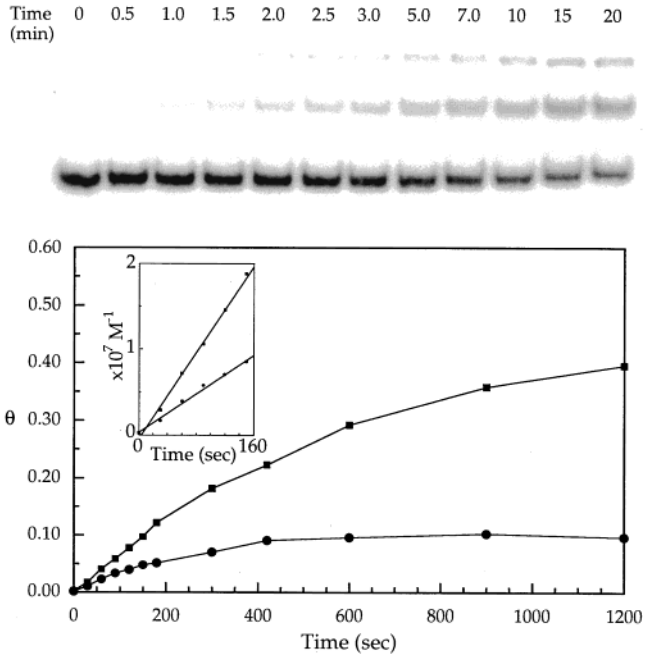

FIGURE 4: Representative EMSA experiment to determine k_{on}. The binding reaction was initiated by addition of protein. Aliquots were quenched by addition of poly[dI·dC] competitor and immediately subjected to native gel electrophoresis (top). The lower band is free DNA and the upper band (growing in with time) is the DNA−TBP complex. The gel displays results for the Pt_2[−4,+4] probe. The plot (bottom) shows the fraction of bound DNA versus time for an unplatinated ([−4,+4], circles) and a platinated (Pt_2[−4,+4], squares) probe. The linear part of the reaction was fit to eq 4 (inset) to obtain k_{on} as the slope of the line.

Table 2: Kinetic Parameters and Binding Constants for yTBP−DNA Complexes

abbreviation	k_{on} (M^{-1} s^{-1})[a]	k_{off} (s^{-1})[a]	K_d (M)
[−5,+5]	$3.1 \pm 0.4 \times 10^4$	$1.3 \pm 0.2 \times 10^{-4}$	4.2×10^{-9}
Pt_2[−5,+5]	$1.5 \pm 0.6 \times 10^5$	$7.1 \pm 0.3 \times 10^{-5}$	4.7×10^{-10}
[−4,+5]	$2.0 \pm 0.3 \times 10^4$	$1.1 \pm 0.1 \times 10^{-4}$	5.5×10^{-9}
Pt_2[−4,+5]	$6.9 \pm 1.3 \times 10^4$	$6.5 \pm 0.4 \times 10^{-6}$	9.4×10^{-11}
[−3,+5][b]	n/a	n/a	n/a
Pt_2[−3,+5]	$6.8 \pm 1.4 \times 10^4$	$9.2 \pm 0.4 \times 10^{-5}$	1.4×10^{-9}
[−4,+4]	$3.8 \pm 1.0 \times 10^4$	$1.2 \pm 0.1 \times 10^{-4}$	3.2×10^{-9}
Pt_2[−4,+4]	$1.1 \pm 0.2 \times 10^5$	$3.9 \pm 0.3 \times 10^{-6}$	3.5×10^{-11}
^{3}Pt[−4,+4]	$1.9 \pm 0.4 \times 10^5$	$3.4 \pm 0.4 \times 10^{-6}$	1.8×10^{-11}
^{5}Pt[−4,+4]	$2.1 \pm 0.4 \times 10^5$	$4.9 \pm 0.7 \times 10^{-6}$	2.3×10^{-11}

[a] Errors indicate one standard deviation. [b] Binding was too weak to obtain reliable data.

21, *22*). The [−3,+5] probe forms such a weak complex with yTBP due to the mutated sequence GATAAA that it was not possible to obtain a reliable K_d value under the experimental conditions employed.

The stability of TBP complexes of the platinum-modified probes was higher than for the corresponding unmodified probes but varied substantially because of k_{off} depending on the position of the platinum adducts with respect to the TATA element. Complex stability was maximized when the platinum adduct was located at the [−4,+N] or [−N,+4] positions. No additional stability was obtained by having two platinum adducts on both sides of the TATA box when compared with probes having only one platinum at either the 5′- or 3′-side. This lack of augmented stability suggests that the structural distortions caused by cisplatin adducts do not contribute to protein binding in a cooperative manner.

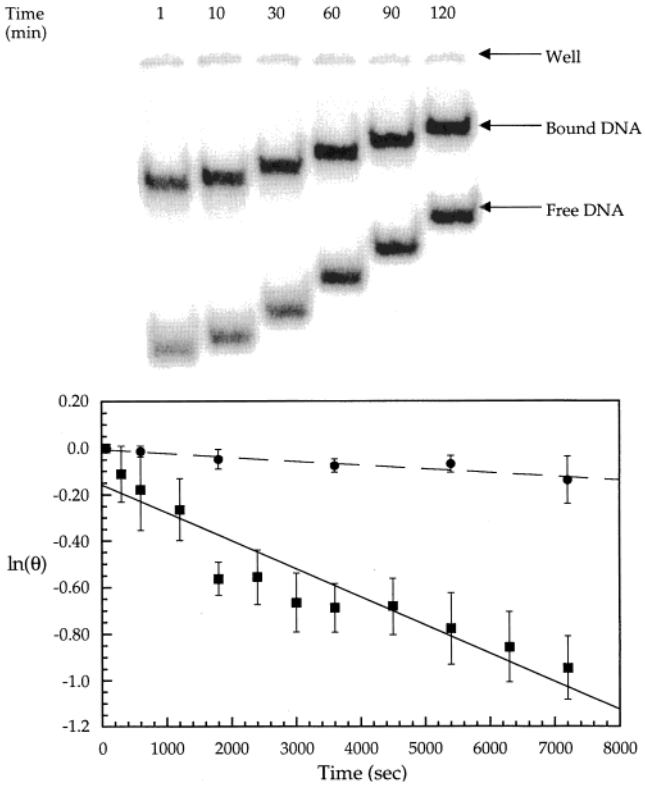

FIGURE 5: A representative EMSA experiment to determine k_{off}. The binding reaction was incubated for 1 h before addition of poly-[dI·dC] competitor. The gel (top) shown is with Pt_2[−4,+4] probe. The times shown above the gel represent the time after addition of competitor, at which point an aliquot of the reaction mixture (20 μL) was resolved by gel electrophoresis. Loss in the fraction of bound DNA (upper band in each lane) versus time was used to determine the unimolecular dissociation rate constant. The plot (bottom) shows the natural log of the fraction of bound DNA over time (eq 2, see text) for an unplatinated probe ([−4,+4], circles) and a platinated probe (Pt_2[−4,+4], squares).

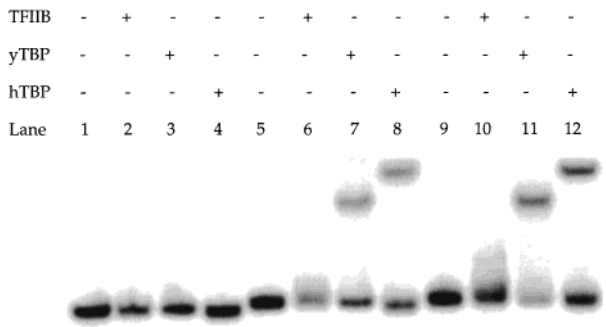

FIGURE 6: EMSA of transcription factors with three TATA box probes. Platinated probes ^{3}Pt[−4,+4] (lanes 5−8) and Pt_2[−4,+4] (lanes 9−12) show increased binding to yTBP and hTBP as compared to the unplatinated probe ([−4,+4], lanes 1−4). TFIIB is not expected to and does not show enhanced binding to platinated probes (lanes 2, 6, and 10), demonstrating the specificity of the TBP enhancement. Total protein concentrations are 44, 1.3, and 13 μg/mL for TFIIB, yTBP, and hTBP, respectively.

Human TBP Binding Enhancement. EMSA was used to examine the binding of full-length human TATA-binding protein (hTBP) and TFIIB to platinum-modified probes (*17*). Figure 6 shows that binding of hTBP to the ^{3}Pt[−4,+4] and Pt_2[−4,+4] probes is increased relative to [−4,+4]. A comparable augmentation is observed for yTBP and hTBP. As anticipated, binding of TFIIB, a protein that does not contain a TATA-binding domain, does not show enhanced

binding to platinated probes. The experiment indicates that platination at flanking sites to the TATA element generally enhances binding for the highly conserved TBP proteins.

DISCUSSION

Design of an Enhanced Binding Site. The initial aim of this study was to use recent structural information obtained for the interaction of HMG domain proteins with cisplatin-modified DNA to prepare an enhanced affinity-binding site for the TATA-binding protein. The structure of HMG1 domain A bound to a cisplatin-modified 16-mer duplex revealed a critical intercalating interaction (*13*). The DNA is kinked at the site of damage, with the adjacent guanine bases destacked due to a large roll (61°) caused by coordination to the platinum atom. This adduct creates an exposed hydrophobic surface or "notch" in the minor grove that receives the intercalating phenylalanine. Intercalating residues are key features of complexes between HMG domains and cisplatin-modified DNA and between TBP and its cognate DNA (*2*, *13*). The TBP intercalating phenylalanine residues were therefore given prime consideration in designing the placement of cisplatin cross-links to form stable complexes with the protein. The engineered binding sites indeed enhance the affinity over unmodified consensus TATA elements. Improved intercalation and predisposed bending of the modified TATA boxes most likely contribute to the enhancement (vide infra). The result is a unique situation in which the designed placement of a DNA-damaging agent enhances the affinity of a DNA-binding protein for its consensus sequence.

Trends in Rate and Dissociation Constants. yTBP clearly binds with enhanced affinity to TATA boxes having cisplatin-modified flanking sequences. Kinetic studies indicate that increased binding is largely a consequence of the diminished dissociation rate constant, not appreciable increases in the association rate constant. Two major trends are apparent in the K_d values. The first is the dependence of K_d on the position of the platinum adducts. Binding enhancement is maximized when the platinum adducts are located at or near the sites of yTBP phenylalanine intercalation, as best illustrated by comparing results for $Pt_2[-5,+5]$ and $Pt_2[-4,+4]$. The latter forms a greater than 10-fold more stable complex as compared with the former. The $Pt_2[-4,+4]$ probe has platinum lesions one base pair removed from (on the 5′-side) and exactly at (on the 3′-side) the sites of phenylalanine intercalation (*4*). The more weakly binding $Pt_2[-5,+5]$ system has platinum adducts located two base pairs from (5′) and adjacent to (3′) the sites of intercalation.

The second important feature of the K_d values is the inability of a second platinum adduct to enhance TBP binding as compared with a single flanking platinum lesion. Probes containing only one platinum adduct, $^5Pt[-4,+4]$ and $^3Pt[-4,+4]$, both stabilize the yTBP−DNA complex to a degree comparable to the two-platinum system ($Pt_2[-4,+4]$). The data indicate that yTBP gains stability predominantly from the presence of just one platinum adduct and suggest that, when a second adduct is present, it is not positioned for intercalative binding in such a manner to stabilize further the complex.

Implications for Drug Design. Recognition of cisplatin damage by TBP prompted the suggestion that the protein should be considered in future drug design (*15*). TBP binding is largely facilitated by hydrophobic interactions at a widened and flattened minor groove in addition to two sites of intercalation where sharp kinks are induced in the DNA. These structural parameters suggest that a rational approach to drug design might include the synthesis of tethered bisplatinum (*23*−*25*) compounds to modify DNA and target TBP specifically. Such compounds could be prepared to facilitate the formation of platinum lesions with the correct spacing to enhance intercalative interactions. Cisplatin cross-links unwind DNA, creating a wide, shallow minor groove with enhanced hydrophobic surface area. Our results suggest that this kind of directed design to target TBP may not be advantageous. The stability of the DNA−TBP complexes indicates that a single platinum adduct placed at the site of intercalation of a TATA element is sufficient to produce a 175-fold increase in affinity but that a second platinum adduct offers no significant enhancement in complex stability. The presence of two platinum adducts in proximity (less than 7-bp separation) to one another may simply create a DNA structure that is too severely distorted for effective TBP binding. We conclude that cisplatin 1,2-intrastrand cross-links may be sufficient to hijack TBP from its native binding site and that future studies should focus on elucidating the precise structure, stability, and cellular consequences of such interactions.

Relevance to Cisplatin Toxicity. The retinoic acid β gene promoter sequence is preferentially platinated as compared to the coding region of the gene in T47D breast cancer cells when the gene is activated with retinoic acid (*26*). Enhanced platination of promoter regions containing a TATA box has only been observed during promoter activation, when localization of TBP and other preinitiation complex (PIC) proteins is most significant. If the promoter region and TATA elements are hypersensitive to platination during activated transcription, then lesions similar to those presented here may exist in vivo. The direct biological consequence of such lesions is not clear, but the formation of highly stabilized TBP complexes could result in unregulated transcription of damaged promoters due to an inability to execute promoter clearance (*1*). Another possibility is that enhanced TBP binding could affect the ability of the protein to make critical protein−protein interactions, thereby disrupting transcription. The former hypothesis is supported by the ability of TFIIB to supershift complexes of TBP with $^3Pt[-4,+4]$ and $Pt_2[-4,+4]$ in native gels not containing $MgCl_2$ (data not shown), indicating that additional transcription factors can interact with platinum-stabilized TBP−DNA assemblies (*27*).

Transcription initiation of RNA polymerase II is inhibited by cisplatin in a concentration-dependent fashion (*28*). Cisplatin damage can titrate yTBP from promoter sites, thereby disrupting transcription in vitro (*15*). yTBP also binds to cisplatin-modified DNA in bandshift and nitrocellulose binding assays. Additional studies indicate that yTBP binds specifically to 1,2-intrastand d(GpG) adducts (*14*). These observations, combined with the strong binding enhancements in the systems presented here, suggest that binding of TBP to cisplatin lesions could be important for its biological activity. Moreover, our data offer the first quantitative information about the binding of TBP to cisplatin-modified DNA. As a critical housekeeping protein, TBP may be hijacked from appropriate promoter sites, disrupting vital

gene transcription. The experiments suggest that the high affinity of TBP for cisplatin-damaged DNA could also serve to shield platinum adducts from DNA excision repair (*12*).

Cisplatin has proved particularly successful for treating testicular cancer (*10*). Studies have focused on testis-specific HMG or on the HMG domain protein SRY to elucidate the unique efficacy of cisplatin against these tumors (*29*, *30*). TBP mRNA is 1000-fold overexpressed in spermatids over somatic cells (*31*, *32*). Whether or not this mRNA is translated into protein is currently unknown, but such a large excess of this protein may not be required in transcription initiation. It is tempting to speculate that the excess of highly overexpressed TBP may perform a secondary function in spermatids that would also render it kinetically available to bind to cisplatin-modified DNA. The resultant complexes could either divert TBP from such important functions and/or may protect the cisplatin damage from repair, allowing the lesion to persist and trigger tumor cell death.

ACKNOWLEDGMENT

We thank Prof. J. D. Parvin for providing a gift of yTBP, vectors contain yTBP and hTBP, and many helpful discussions; Prof. P. A. Sharp and Dr. D. Dykxhoorn for providing a gift of TFIIB and hTBP; Q. He, A. T. Yarnell, and Dr. S. S. Marla for technical assistance and helpful discussions; and Johnson Matthey for a gift of cisplatin.

SUPPORTING INFORMATION AVAILABLE

Detailed sequence and synthetic schemes for oligonucleotide probes. Table of mass spectra data for platinated oligonucleotides. SDS−PAGE of purified yTBP. This material is available free of charge via the Internet at http://pubs.acs.org.

REFERENCES

1. Orphanides, G., Lagrange, T., and Reinberg, D. (1996) *Genes Dev. 10*, 2657−2683.
2. Juo, Z. S., Chiu, T. K., Leiberman, P. M., Baikalov, I., Berk, A. J., and Dickerson, R. E. (1996) *J. Mol. Biol. 261*, 239−254.
3. Tan, S., Hunziker, Y., Sargent, D. F., and Richmond, T. J. (1996) *Nature 381*, 127−134.
4. Kim, Y., Geiger, J. H., Hahn, S., and Sigler, P. B. (1993) *Nature 365*, 512−520.
5. Kim, J. L., Nikolov, D. B., and Burley, S. K. (1993) *Nature 365*, 520−527.
6. Nikolov, D. B., Chen, H., Halay, E. D., Usheva, A. A., Hisatake, K., Lee, D. K., Roeder, R. G., and Burley, S. K. (1995) *Nature 377*, 119−128.
7. Parvin, J. D., McCormick, R. J., Sharp, P. A., and Fisher, D. E. (1995) *Nature 373*, 724−727.
8. Grove, A., Galeone, A., Yu, E., Mayol, L., and Geiduschek, E. P. (1998) *J. Mol. Biol. 282*, 731−739.
9. Grosschedl, R., Giese, K., and Pagel, J. (1994) *Trends Genet. 10*, 94−100.
10. Jamieson, E. R., and Lippard, S. J. (1999) *Chem. Rev. 99*, 2467−2498.
11. Gelasco, A., and Lippard, S. J. (1999) in *Topics in Biological Inorganic Chemistry* (Clarke, M., Sadler, P. J., Eds.) pp 1−43, Springer-Verlag, Heidelberg.
12. Zamble, D. B., and Lippard, S. J. (1999) in *Cisplatin-Chemistry and Biochemistry of a Leading Anticancer Drug* (Lippert, B., Ed.) pp 73−110, Verlag Helvetica Chimica Acta, Zurich.
13. Ohndorf, U.-M., Rould, M. A., He, Q., Pabo, C. O., and Lippard, S. J. (1999) *Nature 399*, 708−712.
14. Coin, F., Frit, P., Viollet, B., Salles, B., and Egly, J.-M. (1998) *Mol. Cell. Biol. 18*, 3907−3914.
15. Vichi, P., Coin, F., Renaud, J.-P., Vermeulen, W., Hoeijmakers, J. H. J., Moras, D., and Egly, J.-M. (1997) *EMBO J. 16*, 7444−7456.
16. Starr, D. B., Hoopes, B. C., and Hawley, D. K. (1995) *J. Mol. Biol. 250*, 434−446.
17. Maldonado, E., Drapkin, R., and Reinberg, D. (1996) *Methods Enzymol. 274*, 72−100.
18. Chasman, D. I., Flaherty, K. M., Sharp, P. A., and Kornberg, R. D. (1993) *Proc. Natl. Acad. Sci. U.S.A. 90*, 8174−8178.
19. Hahn, S., Buratowski, S., Sharp, P. A., and Guarente, L. (1989) *Proc. Natl. Acad. Sci. U.S.A. 86*, 5718−5722.
20. Wobbe, C. R., and Struhl, K. (1990) *Mol. Cell. Biol. 10*, 3859−3867.
21. Hoopes, B. C., LeBlanc, J. F., and Hawley, D. K. (1992) *J. Biol. Chem. 267*, 11539−11547.
22. Kuddus, R., and Schmidt, M. C. (1993) *Nucleic Acids Res. 21*, 1789−1796.
23. Qu, Y., Bloemink, M. J., Reedijk, J., Hambley, T. W., and Farrell, N. (1996) *J. Am. Chem. Soc. 118*, 9307−9313.
24. Zou, Y., Van Houten, B., and Farrell, N. (1994) *Biochemistry 33*, 5404−5410.
25. Kaŝpárková, J., Mellish, K. J., Qu, Y., Brabec, V., and Farrell, N. (1996) *Biochemistry 35*, 16705−16713.
26. Haghighi, A., Lebedeva, S., and Gjerset, R. A. (1999) *Biochemistry 38*, 12432−12438.
27. Bernués, J., Carrera, P., and Azorín, F. (1996) *Nucleic Acids Res. 24*, 2950−2958.
28. Cullinane, C., Mazur, S. J., Essigmann, J. M., Phillips, D. R., and Bohr, V. A. (1999) *Biochemistry 38*, 6204−6212.
29. Ohndorf, U.-M., Whitehead, J. P., Raju, N. L., and Lippard, S. J. (1997) *Biochemistry 36*, 14807−14815.
30. Trimmer, E. E., Zamble, D. B., Lippard, S. J., and Essigmann, J. M. (1998) *Biochemistry 37*, 352−362.
31. Schmidt, E. E., Ohbayashi, T., Makino, Y., Tamura, T., and Schibler, U. (1997) *J. Biol. Chem. 272*, 5326−5334.
32. Schmidt, E. E., and Schibler, U. (1997) *Dev. Biol. 184*, 138−149.

BI0004495